EPJ Web of Conferences **75**, 03007 (2014)
DOI: 10.1051/epjconf/ 20147503007

Magnetic, electrical and structural properties of annealed ferromagnetic $(Zn,Sn)As_2$:Mn thin films on InP substrates: comparison with undoped $ZnSnAs_2$

N.Uchitomi[1a], H.Oomae[1], H.Toyota[1], K.Yamagami[1], and T.Kambayashi[1]

[1]Department of Electrical Engineering, Nagaoka University of Technology, Niigata, Japan

Abstract. We report the magnetic and electrical properties in Mn-doped and undoped $(Zn,Sn)As_2$ epilayers, that were annealed at slightly higher temperatures than the growth temperature. $(Zn,Sn)As_2$:Mn were epitaxially grown on InP (001) substrates at 300°C, and showed room-temperature ferromagnetism. The hole concentration, saturation magnetization and Curie temperature were measured and evaluated as a function of annealing temperature. The Curie temperature had a tendency to slightly increase at annealing temperatures up to 340°C, and completely disappeared at 400°C. The ferromagnetism could be attributed to hole-mediated ferromagnetism resulting from Mn ion substitutions at both the II-group Zn and IV-group Sn sites, especially from the large solubility of Mn^{2+} substitution at Zn sites. The disappearance of ferromagnetism may be explained by several types of mechanisms : migration of mobile interstitial Mn atoms, diffusion of substitutional Mn ions to the surface, substitution of interstitial Mn atoms on Zn vacancies, and formation of MnAs clusters. It is noteworthy that the growth of magnetic semiconductor thin films from substrate lattice matching is essential for avoiding magnetic secondary phases such as MnAs clusters.

1 Introduction

III-V based diluted magnetic semiconductors (Ga,Mn)As have been extensively studied from both experimental and theoretical viewpoints in attempts to achieve a higher Curie temperature [1-3]. In particular, post-growth annealing in temperatures only slightly exceeding a growth temperature of molecular beam epitaxy (MBE) has been performed as an effective means of enhancing the Curie temperature of (Ga,Mn)As by removing Mn interstitial atoms, since Mn interstitials incorporated during low-temperature MBE growth act as double donors that compensate for holes introduced by substitutional Mn_{Ga} [4-5].

As alternative ferromagnetic semiconductors, II-IV-V_2 based semiconductors such as $CdGeP_2$,[6] and $ZnSnAs_2$ [7] have been shown to become ferromagnetic by Mn doping, and have Curie temperatures higher than 300 K. Magnetic properties of several kinds of chalcopyrites including $ZnSnAs_2$:Mn were also theoretically investigated by Kent and Schulthess, who found that $ZnSnAs_2$:Mn has a preference for anti-ferromagnetic interaction with Mn_{II} - Mn_{II} pairs and for ferromagnetic interaction with Mn_{II} - Mn_{IV} and Mn_{IV} - Mn_{IV} site pairs. The magnetic ion Mn, which occupies the cation IV site in host chalcopyrite or zinc-blende (sphalerite) structures, has a local spin and at the same time acts as an acceptor [8]. Very recently, $ZnSnAs_2$:Mn thin films have been epitaxially grown on InP (001) without any secondary phases, and showed room-temperature ferromagnetism [9,10]. Until now the effect of thermal annealing on the transport and magnetic properties of (Ga,Mn)As has been widely studied to improve its magnetic properties and crystallinity and to enhance the Curie temperature up to room temperature. $(Zn,Sn)As_2$:Mn, as well as (Ga,Mn)As, is expected to offer opportunities for systematic investigations of magnetic and electrical properties, especially the influence of thermal annealing on ferromagnetism, both experimentally and theoretically. $(Zn,Sn)As_2$ is probably regarded as a "vertical GaAs" to some extent, consisting of two interposing zinc-blende lattices, and permits a high degree of Mn incorporation because Mn^{2+} ions easily substitute on the group II Zn sites. $(Zn,Sn)As_2$ thin films grown by MBE tend to show zinc-blende structure rather than chalcopyrite structure, which is analogous to the GaAs zinc-blende structure with Ga atoms being randomly replaced with either a Zn or an Sn atom.

In this paper, we investigated the effect of thermal annealing on the electrical and magnetic properties of $(Zn,Sn)As_2$:Mn thin films together with undoped $(Zn,Sn)As_2$ thin films in order to understand the relationship between thermal treatments and their magnetic properties. We compared our results with the extensive experimental and theoretical results for

[a] Corresponding author : uchitomi@nagaokaut.ac.jp

(Ga,Mn)As thin films to explain the magnetic properties of (Zn,Sn)As_2:Mn thin films.

2 Experimental procedures

(Zn,Sn)As_2 films doped with a 12 % Mn content were mainly employed for this experiment. The (Zn,Sn)As_2:Mn films were grown on semi-insulating InP (001) substrates in an MBE chamber using solid elemental sources. Using the optimum substrate temperature of 300 °C and a Zn:Sn:As_4 beam equivalent pressure (BEP) ratio of 24:1:52, we grew a 100-nm thick (Zn,Sn)As_2 epitaxial film doped with a nominal 12 % Mn on a 16-nm (Zn,Sn)As_2 buffer layer. The detailed growth procedure of (Zn,Sn)As_2:Mn films on InP (001) has been published elsewhere [9]. The as-grown sample was cleaved into several pieces for annealing at temperatures of 310, 320, 340 and 400°C using face-to-face proximity capping by GaAs wafers to simulate an arsenic atmosphere in order to inhibit surface degradation outside the MBE chamber. High-resolution X-ray diffraction (HR-XRD) measurements were performed to investigate the lattice constant variation of annealed samples. Magnetic properties were determined by vibrating sample magnetometer measurement, and electrical properties were determined by Hall measurements. We preliminarily investigated the influence of annealing times of 10, 60 and 120 min on magnetization in (Zn,Sn)As_2 films with a 7 % Mn content at 320°C in order to determine the appropriate annealing time. It was found that the field-dependent magnetization observed at 10 K using superconducting quantum interference device (SQUID) magnetometry was almost independent of annealing time up to 120 min. From the preliminary experiment, the longest annealing time of 120 min was selected for the present experiment.

3 Results and discussion

Figure 1 shows $\theta - 2\theta$ high-resolution X-ray diffraction (XRD) patterns of the as-grown sample and samples annealed at temperatures slightly higher than the growth temperature of 300°C. The $\theta - 2\theta$ wide scans as shown in Fig. 1 (a)-(e) were examined to determine whether they detected peaks of secondary MnAs crystals in the annealed samples formed by thermal annealing process at several orders of logarithmic scales. The presence of secondary MnAs clusterings was likely beyond the detection limit of XRD measurements. Figure 1 (f)-(i) shows $\theta - 2\theta$ high-resolution XRD patterns recorded across the InP (004) substrate reflection. The peak of (Zn,Sn)As_2:Mn was observed very close to the peak of InP (004) reflection. To compare the diffraction peak shifts of (Zn, Sn)As_2:Mn thin films with the case of undoped samples, $\theta - 2\theta$ high-resolution XRD patterns of the undoped as-grown sample and samples annealed at temperatures slightly higher than the growth temperature of 300°C were also examined (not shown here). The undoped (Zn,Sn)As_2 thin films were confirmed to show

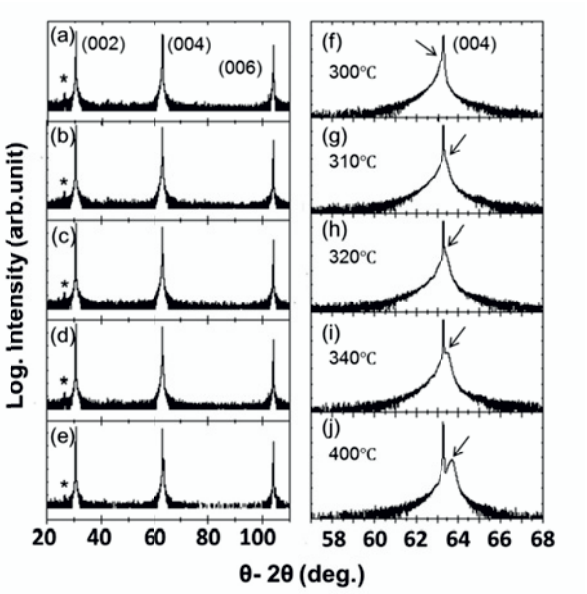

Figure 1. (a) - (e) Wide-scan $\theta - 2\theta$ high-resolution X-ray diffraction patterns of $ZnSnAs_2$:Mn thin films as a function of annealing temperature. The asterisk corresponds to the peak of $ZnSnAs_2$ (112) reflection. (f) – (j) Narrow-scan $\theta - 2\theta$ high-resolution X-ray diffraction patterns around InP (004) reflection of $ZnSnAs_2$ thin films.

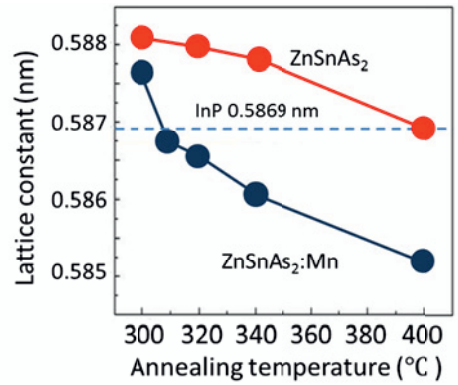

Figure 2. Lattice constants of $ZnSnAs_2$ and $ZnSnAs_2$:Mn films as a function of annealing temperature.

high-qualtiy crystallinity. In the case of (Zn,Sn)As_2:Mn on InP substrates, the lattice mismatch of the as-grown sample with the substrate was initially 0.03 %. As the annealing temperature increased, the (Zn,Sn)As_2:Mn diffraction peak shifted towards the higher Bragg angle. Figure 1 indicates that upon annealing at 310°C, the positive lattice mismatch decreased to zero and eventually increased negatively with increasing annealing temperatures. The value of the full width at half maximum (FWHM) observed for a 400°C-annealed sample was slightly larger than those observed for samples annealed at 310 - 340°C, which showed degradation of their crystallinity above 340°C.

The lattice constants of (Zn,Sn)As_2:Mn films are plotted as a function of annealing temperature in Fig 2. As seen in the figure, the lattice constant decreased monotonically with temperature, and crossed the line of the InP lattice constant at 310°C. The (Zn,Sn)As_2:Mn film on the InP

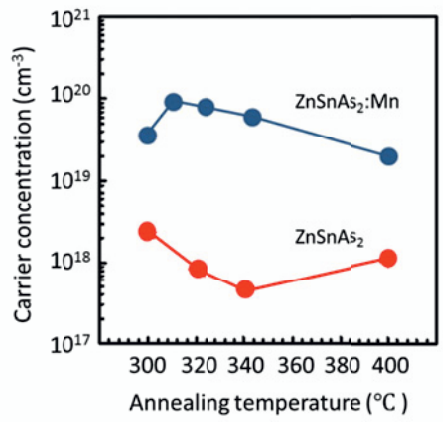

Figure 3. Hole carrier concentration of $ZnSnAs_2$ and $ZnSnAs_2$:Mn films as a function of annealing temperature.

substrate is under compressive strain, and changes in response to tensile strain depending on the annealing conditions. On the other hand, the lattice constant of undoped (Zn,Sn)As_2 fims decreased gradually towards the lattice constant of InP with increasing annealing temperature to 400°C.

Figure 3 shows the effect of annealing temperature on carrier concentration of $ZnSnAs_2$:Mn thin films together with $ZnSnAs_2$ thin films. The hole concentration of $ZnSnAs_2$:Mn was 1-2 orders of magnitude larger than that of ZnSnAs2 because the Mn atoms act as acceptors, leading effectively to carrier-mediated ferromagnetism.

Figure 4 shows the remanent magnetization as a function of applied magnetic field with respect to each annealing temperature. It was found that these *M-T* curves clearly showed Curie temperatures more than 300 K. The *M-T* curve then disappeared at a annealing temperature of 400 °C.

Figure 5, 6 and 7 display the effect of annealing temperature on Curie temperature, carrier concentration, and saturation magnetization. The saturation magnetization at 77 K and the Curie temperature were determined from *M-T* curves. The hole concentration and saturation magnetization showed maximum values of 8.26×10^{19} cm^{-3} and 84 emu/cm^3 at 310°C, which was slightly higher than growth temperature, and then decreased gradually, disappearing at 400°C. From these results, we found a good correlation between the temperature-dependent hole concentration and saturation magnetization. In the case of (Ga,Mn)As, it is well-known that the Curie temperature and the saturation magnetization are significantly enhanced by low-temperature annealing ; with annealing above the optimal temperature (typically around 300°C), both the Curie temperature and the saturation magnetization are seen to decrease monotonically. The annealing of (Ga,Mn)As leads to a dramatic drop of *Tc* to a value below that of the as-grown sample. In contrast to the case of the (Ga,Mn)As, the Curie temperature of (Zn,Sn)As_2:Mn films does not seem to strongly depend on annealing temperatures around 340°C.

The thermal behavior of electrical and magnetic properties in (Zn,Sn)As_2:Mn thin films as a function of

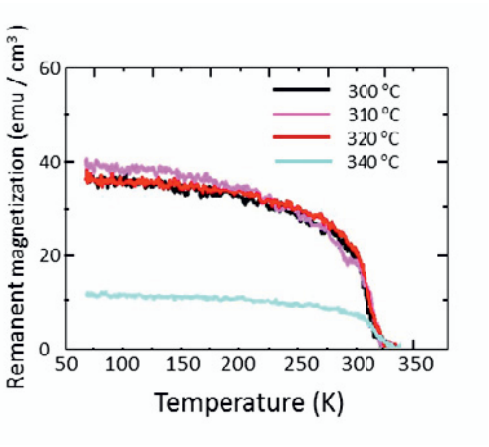

Figure 4. Temperature dependence of the remanent magnetization for as-grown and annealed samples of 12% Mn-doped (Zn,Sn)As_2 films.

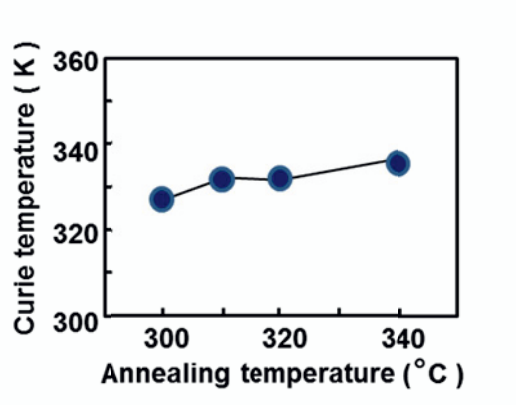

Figure 5 Curie temperature as a function of annealing temperature.

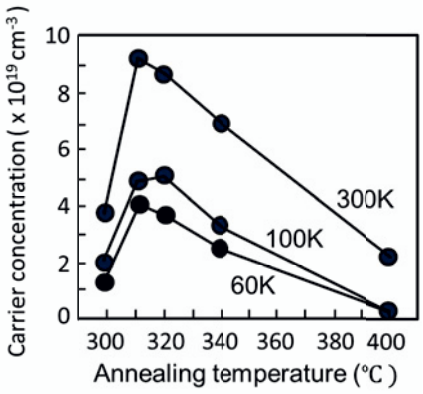

Figure 6. Hole carrier concentration measured at 60, 100, and 300 K as a function of annealing temperature.

annealing temperature could be explained by several different types of mechanisms such as the migration of mobile interstitial Mn atoms, the diffusion of substitutional Mn ions to the surface, the substitution of interstitial Mn atoms on Zn vacancies, and the formation of MnAs clustering. The room-temperature ferromagnetism in Mn-doped chalcopyrite semiconductors such as $CdSnP_2$:Mn bulk materials has

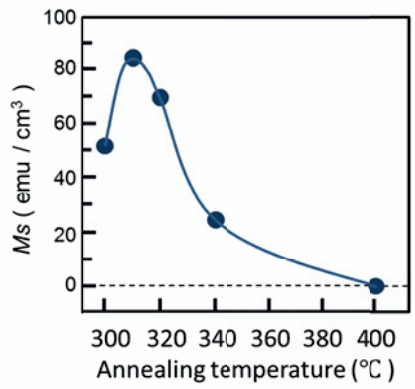

Figure 7. Variation of saturation magnetization at 77 K, as a function of annealing temperature.

.

raised the question whether ferromagnetic properties are intrinsic, or due to phase segregation [11]. Their observations suggested that the ferromagnetic behavior arises from MnAs or MnP secondary phases that were formed in the synthesized bulk-chalcopyrite matrix. On the basis of these suggestions, the origin of ferromagnetism in chalcopyrites is complicated and seems in some extent to be related to local structures of As-Mn-As. Therefore, careful attention must be paid to the interpretation of whether the ferromagnetic response is due to intrinsic semiconductor nature or to secondary phase formations such as MnAs clusters with ferromagnetic transition temperatures of around 320 K. As for the (Zn,Sn)As_2 :Mn thin film, this material closely lattice-matched to InP substrates, as well as a (Ga,Mn)As thin film on GaAs substrates. This means that the lattice-match between magnetic semiconductors and substrates is a crucial factor to eliminate the possible formation of magnetic secondary phases such as MnAs clusters. The XRD measurements of (Zn,Sn)As_2 :Mn thin films revealed no visible secondary-phase MnAs on a logarithmic scale, and SQUID measurements revealed no blocking temperature. In addition, an anomalous Hall effect was clearly observed [10], which plays a very important role in diluted magnetic semiconductors. On the basis of these experimental results, the thermal effect of $ZnSnAs_2$:Mn could be explained assuming that the magnetic properties are caused by semiconducting properties with Mn magnetic atoms.

It is likely that the migration of interstitial Mn atoms in $ZnSnAs_2$:Mn leads to the decrease of the lattice constant by analogy to (Ga,Mn)As as shown in Fig. 2. On this assumption, its diffusion length would be proportional to the difference of the lattice constant Δd observed at each annealing temperature T. The activation energy Q for the activation of interstitial Mn atoms to the surface may be estimated from the Arrhenius plot of Δd vs. $1/T$. Assuming $\Delta d \propto \exp(-Q/2kT)$, we estimated the Q to be 1.16 eV. Compared with these experimental and theoretical works for the activation energy of Mn interstitials in (Ga,Mn)As [12,13], the activation energy of (Zn,Sn)As_2:Mn seems to be reasonable. Therefore, the diffusion mechanism of Mn interstitials in (Zn,Sn)As_2:Mn could be explained by a similar framework as that of the zinc-blende (Ga,Mn)As structure except for the presence of two interstitial sites.

5 Conclusion

We report the first experimental results of magnetic and electrical properties in (Zn,Sn)As_2 :Mn epilayers annealed at slightly higher temperatures than the growth temperature. (Zn,Sn)As_2:Mn was epitaxially grown on InP (001) substrates at 300°C, and showed room-temperature ferromagnetism. The hole concentration, saturation magnetization and Curie temperature were measured and evaluated as a function of the annealing temperature. We found that the Curie temperature showed stable values of around 331 K for annealing temperatures up to 340°C. Its disappearance at 400°C could be explained by several mechanisms: migration of mobile interstitial Mn atoms, diffusion of substitutional Mn ions to the surface, substitution of interstitial Mn atoms on Zn vacancies, and formation of MnAs clustering.

References

1. H.Ohno, Science **281**, 951 (1998)
2. T. Dietl, H. Ohno, and F. Matsukura, Phys. Rev. **B 63**, 195205 (2001).
3. S.Sato, M.A.Osman, Y.Jinbo, and N.Uchitomi, Appl.Surf. Sci. **242** 134 (2005).
4. T.Hayashi, Y.Hashimoto, S.Katsumoto, Y.Iye, Appl. Phys. Lett. **78**, 1691 (2001).
5. S.J.Potashnik, K.C.Ku, S.H.Chun, J.J.Berry, N.Samarth, P.Schiffer, Appl.Phys.Lett. **79**, 1495 (2001).
6. G.A.Medvedkin, T.Ishibashi, T.Nishi, K.Hayata, Y.Hasegawa, and K.Sato, Jpn.J.Appl.Phys. **39**, L949 (2000).
7. S.Choi, G.B.Cha, S.C.Hong, S.Cho, Y.Kim, J.B.Ketterson, S.Y.Jeong, and G.C.Yi, Solid State Commun. **122**, 165 (2002).
8. P.R.C.Kent, T.C.Schulthess, AIP Conf. Proc. **772**, (2005) 1369..
9. J.T.Asubar, Y.Jinbo, N.Uchitomi, J. Crys. Growth **311,** 929 (2009).
10. H. Oomae, J. T. asubar, Y. Jinbo, N.Uchitomi, Jap. J. Appl. Phys.. **50**, 01BE12 (2011)
11. J.Adell, I.Ulfat, L.Ilver, J.Sadowski, K.Karlsson, J.Kanski, J.Phys: Condens. Matter, **23**, 085003 (2011)
12. K.W.Edmonds, P.Bogustawshi, K.Y.Wang, R.P.Campion, S.N.Novikov, N.R.S.Farley, B.L.Gallagher, C.T.Foxon, M.Sawicki, T.Dietl, M.Buongiorno Nardelli, J.Bernhole, Phys. Rev. Lett. **92**, 037201 (2004)
13. M.Wang, R.P.Campion, A.W.Rushforth, K.W.Edmonds, C.T.Foxon, B.L.Gallagher, , Appl. Phys. Lett. **93**, 132103 (2008).